HHS Public Access

Author manuscript

Exp Eye Res. Author manuscript; available in PMC 2020 November 01.

Published in final edited form as:

Exp Eye Res. 2019 November ; 188: 107798. doi:10.1016/j.exer.2019.107798.

Novel Anti-Angiogenic PEDF-Derived Small Peptides Mitigate Choroidal Neovascularization

Nader Sheibani[1], **Shoujian Wang**[1], **Soesiawati R. Darjatmoko**[1], **Debra L. Fisk**[1], **Pawan K. Shahi**[2], **Bikash R. Patnaik**[2], **Christine M. Sorenson**[2], **Reshma Bhowmick**[3,*], **Olga V. Volpert**[3,*], **Daniel M Albert**[1,*], **Ignacio Melgar-Asensio**[4], **Jack Henkin**[4]

[1]Departments of Ophthalmology and Visual Sciences, Biomedical Engineering, and Cell and Regenerative Biology, University of Wisconsin School of Medicine and Public Health, Madison, WI

[2]Department of Pediatrics, University of Wisconsin School of Medicine and Public Health, Madison, WI

[3]Department of Urology, Feinberg School of Medicine, Northwestern University, Chicago, IL

[4]Center for Developmental Therapeutics, Northwestern University, Evanston IL

Abstract

Abnormal migration and proliferation of endothelial cells (EC) drive neovascular retinopathies. While anti-VEGF treatment slows progression, pathology is often supported by decrease in intraocular pigment epithelium-derived factor (PEDF), an endogenous inhibitor of angiogenesis. A surface helical 34-mer peptide of PEDF, comprising this activity, is efficacious in animal models of neovascular retina disease but remains impractically large for therapeutic use. We sought smaller fragments within this sequence that mitigate choroidal neovascularization (CNV). Expecting rapid intravitreal (IVT) clearance, we also developed a method to reversibly attach peptides to nano-carriers for extended delivery. Synthetic fragments of 34-mer yielded smaller anti-angiogenic peptides, and N-terminal capping with dicarboxylic acids did not diminish activity. Charge restoration via substitution of an internal aspartate by asparagine improved potency, achieving low nM apoptotic response in VEGF-activated EC. Two optimized peptides (PEDF 335, 8-mer and PEDF 336, 9-mer) were tested in a mouse model of laser-induced CNV. IVT injection of either peptide, 2–5 days before laser treatment, gave significant CNV decrease at day +14 post laser treatment. The 8-mer also decreased CNV, when administered as eye drops. Also examined was a nanoparticle-conjugate (NPC) prodrug of the 9-mer, having positive zeta

Correspondence to: Jack Henkin, Center for Developmental Therapeutics, Northwestern University, Silverman Hall, Evanston IL, 60208 j-henkin@northwestern.edu.

*Denotes:Present address RB: Department of Thoracic and Cardiovascular Surgery, MD Anderson Cancer Center, Houston, TX 77030
OVV: Department of Cancer Biology, MD Anderson Cancer Center, Houston, TX 77054
DMA: Department of Ophthalmology, Casey Eye Institute, Oregon Health Sciences University, Portland, OR, 97239

Financial dislosures

NS, SW, SRD, DLF, PKS, BRP, CMS, RB, and DMA have no financial disclosures. JH, OVV, and IMA are listed inventors on an issued US patent covering described peptides, assigned to Northwestern University (NU). JH and IMA are listed inventors on a pending patent application describing a nanoparticle delivery system (Figure 6), assigned to NU.

potential, expected to display longer intraocular residence. This NPC showed extended efficacy, even when injected 14 days before laser treatment. Neither inflammatory cells nor other histopathologic abnormalities were seen in rabbit eyes harvested 14 days following IVT injection of PEDF 336 (>200 μg). No rabbit or mouse eye irritation was observed over 12–17 days of PEDF 335 eye drops (10 mM). Viability was unaffected in 3 retinal and 2 choroidal cell types by PEDF 335 up to 100 μM, PEDF 336 (100 μM) gave slight growth inhibition only in choroidal EC. A small anti-angiogenic PEDF epitope (G-Y-**D**-L-Y-R-V) was identified, variants (adipic-Sar-Y-**N**-L-Y-R-V) mitigate CNV, with clinical potential in treating neovascular retinopathy. Their shared active motif, Y - - - R, is found in laminin (Ln) peptide YIGSR, which binds Ln receptor 67LR, a known high-affinity ligand of PEDF 34-mer.

Keywords

angiogenesis; PEDF; choroidal neovascularization; peptides; retinopathy; macular degeneration; laminin receptor; YIGSR

Introduction

Diabetic retinopathy (Willis et al., 2017) and age-related macular degeneration (AMD) are leading causes of blindness in working and elderly populations. The exudative form of AMD, displaying choroidal neovascularization (CNV), progresses most rapidly, with severe impact on vision (Jonasson et al., 2014). Intravitreal (IVT) injection of VEGF-neutralizing proteins is a major advance in slowing these diseases, but 15–30% of patients show poor response or have recurrent CNV (Wolf and Kampik, 2014). VEGF is also an essential survival factor for choroidal endothelial cells (ChEC) and other retinal cells, its chronic inhibition has been associated with undesirable long-term outcomes (Gemenetzi et al., 2017; Wen et al., 2017; Zarubina et al., 2017). Thus, other anti-angiogenic factors, not dependent on VEGF sequestration, are sought to complement current treatment (Sulaiman et al., 2016). The balance between VEGF and other pro- and anti-angiogenic proteins, produced by retinal pigment epithelium (RPE), controls neovascularization. Potent endogenous inhibitors of angiogenesis include thrombospondin-1 (TSP1) and pigment epithelium-derived factor (PEDF) (Farnoodian et al., 2017). A decrease in these protective proteins was found in the Bruch's membrane and RPE of postmortem donor eyes with AMD, compared to age-matched donor eyes without neovascular disease (Uno et al., 2006; Bhutto et al., 2006). PEDF is decreased in diabetic retinopathy (Ogata et al., 2002), it arises late in gestation (Loegl et al., 2016), and is absent in vitreous of premature newborns with retinopathy of prematurity (ROP) (Sugioka et al., 2017).

Secreted PEDF (50 kDa) displays both neuroprotective and anti-angiogenic activities, which are attributed to specific exposed epitopes at the protein surface. A potent angio-inhibitory activity was localized to an α-helical 34-amino acid (aa) segment (34-mer; Asp24-Asn56) (Filleur et al., 2005). IVT administration of PEDF mitigated oxygen induced ischemic retinopathy (OIR) in mice (Duh et al., 2002) and its periocular gene delivery reduced CNV in a laser-induced porcine model (Saishin et al., 2005). The isolated 34-mer itself inhibited laser-induced rat CNV by subconjunctivial injection (Amaral and Becerra, 2010), and its

systemic injection over 5 days decreased OIR in newborn mice (Longeras et al., 2012). The 34-mer, and an N-terminal 25-mer therein has been demonstrated to bind the 67kDa non-integrin laminin (Ln) receptor, 67LR, with high affinity (Bernard et al., 2009). This receptor was displayed in mouse retina during OIR, and a Ln-derived nonapeptide ligand of 67LR mitigated mouse OIR when injected systemically (Gebarowska et al., 2002). Smaller, more C-terminal segments of the PEDF 34-mer (P23 and P18) were found potently anti-angiogenic, and P18 also slowed tumor growth, with reduced tumor microvessel density (Mirochnik et al., 2009).

While bioactive PEDF-peptides ranging from 18–34 residues offer promising potency *in-vivo* against neovascular retinal diseases, their size is still impractical for cost-effective synthesis at high purity. The potential to elicit autoimmune response against PEDF is also of concern. Since major histocompatibility complex (MHC) bind 9–10 mer cores, and bulging loop formation and proteolytic processing in longer peptides can increase antigen presentation and affinity (Yassai etal., 2002), peptides should not extend beyond critical bioactive sequence, ideally <10 aa length in order to minimize immunogenicity. Here we describe a systematic search for smaller peptides, with modifications intended to allow ester prodrug forms for prolonged IVT release. The latter approach was evaluated here, using a peptide-conjugated cationic carrier recently described by our laboratory (Melgar-Asensio et al., 2018). Our studies defined a minimal antiangiogenic sequence of PEDF, and enabled our discovery of small, dicarboxylic acid-modified PEDF peptides, amenable to practical IVT treatment of ocular neovascularization.

2. Materials and Methods

2.1. Peptide Structural Strategy and Synthesis

Structural features of PEDF, and amino acid sequences of its active 34-mer and 23–25 and 18 amino acid peptides therein (Bernard et al., 2009; Mirochnik et al., 2009) are shown in Figure 1A,B. Peptides (>95% pure, 20–50 mg) for *in vitro* evaluation by endothelial cell (EC) apoptosis were custom synthesized by solid state techniques, via N-terminal capping with glutaric and adipic chlorides (CPC Scientific Co., Sunnyvale, CA), and tested *in-vitro.* Candidates for *in-vivo* studies were prepared at >100 mg scale, via Fmoc-based solid-state methods on methylbenzhydrylamine (MBHA) rink amide resin, using a CEM Liberty Blue microwave-assisted peptide synthesizer, at the Peptide Synthesis Core facility of Northwestern University (Simpson Querrey Institute, Chicago, IL). The mono-*tert*-butyl esters of glutaric and adipic acids were appended under standard coupling conditions at 1.5-fold molar excess over 16 h, and *tert*-butyl groups were removed via standard 95% trifluoro-acetic acid (TFA) resin-release. Peptides PEDF 336 and PEDF 335 (Table 1, last 2 peptides) for *in-vivo* use were converted from TFA to hydrochloride salts by 2x lyophilization of 5 mM peptide from 10 mM HCl solution, residual fluorine being shown >98% removed by ^{19}F-NMR. Stock solutions (pH 3.0–3.5) were carefully neutralized to pH 6.5 – 7 with 0.1 M NaOH, or bicarbonate, and lyophilized and sterile filtered after reconstitution with isotonic saline before animal injection.

Adipoyl chloride, and *p*-nitrophenylchloroformate were from Sigma-Aldrich (St. Louis, MO). N-BOC-(R,S)pyrrolidine-3-ol and mono-*tert*-butyl esters of glutaric and adipic acids

were from Alfa-Aesar (Haverhill, MA). Methoxy-PEG_4-amine was from Quanta BioDesign, Plain City, OH. Mono-BOC esters of adipic / glutaric acids were from A1 Biochem Labs (Syracuse, NY).

2.2. Polymer-Conjugated Ester Prodrug of Active Peptide, PEDF 336

Three steps were required to generate a metastable ester-linked NP prodrug of PEDF 336 shown in Figure 1B. These were A: formation of a N-protected 3-pyrrolidinol mono-ester of adipic acid; B: N-terminal capping of the peptide sequence with this adipic half-ester during solid-state peptide synthesis, then deprotection to give a reactive pyrrolidine group; C: carbamate coupling of pyrrolidinol-adipic peptide ester to an activated, condensed polymer of cholesteryl condensed dextran (CDEX).

2.3. Synthesis of BOC-Protected Pyrrolidinol Ester of Adipate; 6-{[1-(tert-Butoxycarbonyl)Pyrrolidin-3-yl]oxy}−6-Oxohexanoic Acid (BPadOH)

N-BOC-(R,S)pyrrolidine-3-ol (1.0 mEq) and triethylamine (TEA) (1.0 mEq) were dissolved in 1 mL dichloromethane (DCM), and added dropwise, over 1–2 min to a solution of 3.0 mEq adipic chloride in 10 mL DCM. After 30 min (RT), the mixture was dried under vacuum, and crude product was dissolved in 25 mL of 1 M sodium bicarbonate. The solution was washed 3x with ethylacetate extraction in a separatory funnel. The aqueous phase pH was adjusted with 1 M HCl to pH 3.5–4.0, the solution then extracted 2x with 50 mL ethyl ether and the organic phase isolated, and dried under vacuum. Final product: BPadOH, was verified by ^{1}H NMR (BOC singlet/ pyrrolidine/ adipic; 9:6:8) and obtained in 47% yield (148 mg).

2.4. Synthesis of Carbamate-Linkable Peptide Ester: Pyrrolidine-3-O-Adipic-N-Sar-Tyr-Leu-Tyr-Arg-Val-Arg-Ser-amide (PE-336)

HN-Sar-YNLYRVRS-rink amide MBHA resin was formed by standard solid state synthetic methods. Then added to 0.25 mmol of this peptide on resin was 0.375 mmol of BPadOH, in *N,N*-dimethylformamide, and followed by 1.45 mEq HATU and 6 mEq of *N,N*-diisopropylethylamine. The reaction mixture was shaken mechanically for 16 h at RT. The resulting peptide was cleaved from the resin using a mixture of 95% TFA, 2.5% water, and 2.5% triisopropylsilane for 3 h. The crude peptide salt was precipitated from this solution using cold diethyl ether before HPLC purification. Solvent evaporation gave the final product, 3-pyrrolidinol ester of PEDF 336: pyrrolidine-3-O-adipic-N-Sar-Tyr-Asn-Leu-Tyr-Arg-Val-Arg-Ser-amide (PE-336), as TFA-salt confirmed by MS (M^+ 1337, white powder), yield 26%.

2.5. Conjugation of the Prodrug Peptide with CDEX-70 NP

The NP used for conjugation of ester-bridged PEDF 336 was CDEX-70, as previously described for stable carbamate attachment of small IVT anchoring peptides (non-ester), linked to CDEX through N-terminal pyrrolidine-PEG_8 (Melgar-Asensio et al., 2018). Here, a metastable ester prodrug, PE-336: pyrrolidinol-adipoyl-Sar-YNLYRVRS-amide, was linked as a carbamate to *p*-nitrophenylchloroformate-activated CDEX. CDEX-(*p*-nP)$_{108}$ (2.2 mg) in 200 μL DMSO was dried under vacuum, then mixed with 4.4 μmoles of PE-336 in

200 μL DMSO, and 11.0 μmoles of TEA was added (1.5 μL) before sealing. The reaction continued for 72 h, at 45°C with rotary shaking. Unreacted *p*-nitrophenyl groups were quenched with 20 μmoles of methoxy-PEG_4-amine at 4°C over 30 min. After dropwise addition of the reaction mixture to aqueous 0.1 M HCl (2 mL) and exhaustive dialysis vs. 0.1 mM HCl, the solution was sterile-filtered and lyophilized. NPC diameter and zeta potential (ζ) in aqueous solution were analyzed in triplicate by dynamic light scattering and electrophoretic light scattering, respectively (Zetasizer Nano ZSP). The ζ, which is derived from direction and velocity of particle motion in an electric field, describes the surface density of charges at the particle's boundary with water. We showed how ζ related inversely to the rate of diffusion of peptide-conjugated compact CDEX spheres in vitreous (Li et al., 2017).

2.6. Loading and Release Rate of PEDF 336 (Ester Hydrolysis, *in-vitro*) from CDEX NPC

NPC in HEPES buffer 100 mM, pH = 7.38 was sterile-filtered and 1.0 mL incubated at 0.37 mg/mL under physiological conditions at 37 °C. Aliquots of 0.30 mL were taken for centrifugal ultrafiltration at time points up to 154 days. Hydrolytically released peptide (PEDF 336) was thus separated (MWCO 10 kDa, 14,000 g, 10 min, RT), from the polymer conjugate of CDEX and PE-336 (carbamate-linked ester prodrug), and UV spectra were obtained for the time-point filtrates (λ = 275 nm) to determine free peptide concentration, PEDF-336 identity was confirmed by HPLC. Initial peptide/NPC load was estimated from the day-154 value, corrected to half-life.

2.7. Endothelial Cell Apoptosis Assay

The assay was performed as described previously (Jimenez et al., 2000). Briefly, primary human dermal microvascular EC (PromoCell-Fisher Scientific) were grown in Endothelial Growth Medium MV (EGM, Fisher Scientific), supplemented with 5% FBS and growth factors (EGM Bullet Kit, Fisher Scientific) and used between passages 3 and 5. For apoptosis induction, EC were cultured overnight in 1% FBS and treated for 48 hours with an increasing concentration of sterile filtered peptides, alone (1–100 nM range) or in combination with VEGF (10 ng/mL). Apoptosis was detected by using terminal deoxynucleotidyl transferase dUTP by nick-end labeling (TUNEL) assay kit according to the manufacturer's instructions (Roche, Indianapolis, IN). The nuclei were counterstained with 4',6-diamidino-2-phenylindole (DAPI). Apoptosis was visualized by fluorescence microscopy (Nikon, Diaphot 2000). Random images were taken at 20x magnification and quantified using Nikon Elements software. Apoptotic fraction or % apoptosis was determined in at least 10 images per condition and the average values calculated. Alternatively, immunostaining for cleaved, active Caspase-3 was used to detect apoptotic cells. Statistical significance was determined using one-way ANOVA.

2.8 *Ex-vivo* Mouse Choroidal Sprouting Assay

Choroidal explant neovascular sprouting assay was carried out as described previously (Shao et al., 2013), with minor modifications. Choroid fragments (1-x-1 mm) were cut from choroids of euthanized C57BL/6J mice ubiquitously expressing EGFP (C57BL/6j-Tg(CAG-EGFP)1Osb/J, Jackson Laboratory, Bar Harbor, ME), stripped of RPE. The fragments were seeded in 24-well plates, and solidified Matrigel drops were immersed in complete EGM

with 5% FCS and growth factors (bullet kit). After 48 h the medium was replaced with serum-free EGM supplemented with VEGF (R&D Systems, 50 ng/mL), with or without peptide and changed every 48 h for 6 days. Sprouting neovasculature was visualized by an epifluorescence microscope (Nikon Diaphot 2000, Nikon) using 4x objective. The composite images generated and the vascular area measured using Nikon Elements software.

2.9. Laser-Induced CNV Experiments

All research using the mouse CNV models was carried out in accordance with the Association for Research in Vision and Ophthalmology Statement for the Use of Animals in Ophthalmic and Vision Research, and was approved by the Institutional Animal Care and Use Committee of the University of Wisconsin School of Medicine and Public Health (Assurance Number, D16–00239). Wild-type 6-week-old female C57BL/6j mice (Jackson Laboratories) were housed on a 12-hour light-dark cycle and provided with food and water ad libitum. The sex of the animals does not impact the outcome of this assay (Gong et al., 2015).

Laser-induced CNV experiments were performed as previously described (Wang et al., 2012). Mice were anesthetized by intraperitoneal injection of ketamine hydrochloride (75 mg/kg) and xylazine (7.5 mg/kg). Pupillary dilation was achieved using tropicamide 1% eye drops. Three bursts of a 532 nm diode laser (75 mm spot size, 0.1 s duration, 120 mW) were delivered to each retina in the 9-, 12-, and 3-o'clock positions. The procedure was performed with the slit lamp delivery system of an OcuLight GL diode laser (Iridex, Mountain View, CA, USA) and a round glass coverslip as a contact lens to view the retina. After euthanizing the mice, eyes were enucleated and fixed in 4% paraformaldehyde at 4°C for 2 h.

After transferring the eyes to PBS, they were sectioned at the equator to obtain posterior sclerochoroidal eyecups. Following incubation in blocking buffer (50% fetal calf serum, 20% normal goat serum and 0.01% Triton-X-100 in PBS) for 1 h at RT, eyecups were incubated with anti-intercellular adhesion molecule-2 antibody (rat-anti-mouse 553326; BD Biosciences, Bedford, MA: 1:500; in blocking buffer) overnight at 4°C. Eyecups were then washed with PBS and incubated with a Cy-3-labeled secondary antibody (donkey-anti-rat, Jackson ImmunoResearch, West Grove, PA, 1:500, in blocking buffer) for 2 h. Afterwards, eyecups were flattened onto a glass slide through 5 to 6 relaxing radial incisions and mounted with VectaMount AQ (Vector Laboratories, Burlingame, CA). Samples were visualized using the 20× objective of an epifluorescent compound microscope fitted with appropriate excitation and emission filters (AxioPhot, Zeiss, Germany). Images were captured using a digital camera (AxioCam, HRm; Zeiss, Oberkochen, Germany) and compatible software (AxioVision 4.8.2, Zeiss). To quantify the total area of CNV associated with each laser spot, ImageJ free-ware was used.

2.10. Toxicity Evaluation of PEDF 335 and 336 Peptides

We performed toxicity evaluation of PEDF 335 and PEDF 336 in mice. The animals received a single IVT injection of 2 μL of 2 mM peptide stocks or balanced salt solution (BSS, Alcon, Fort Worth, TX), and two weeks later they were subjected to

electroretinography (ERG). Following ERG analysis the eyes were harvested and examined by histological evaluation in a masked fashion.

The ERG analysis was performed as previously described by us (Shahi et al., 2017). Mixed ERG were recorded from both sexes and both eyes. Also, same age-sex control animals were recorded from both eyes and served as controls. Before ERG measurement, mice were dark-adapted overnight. Also, all recoding activities were conducted under dim red light. Flash ERG recordings were acquired from both eyes at continual increments of light intensities. Analysis of a-wave and b-wave amplitudes were performed using ERGView analytical software (OcuScience, Henderson, NV). The a-wave amplitude was measured from the baseline to the negative peak, and the b-wave was measured from the a-wave trough to the maximum positive peak and plotted using Origin. These measurements revealed the functional integrity of photoreceptors (a-wave), bipolar cells (b-wave). Data were analyzed off-line using ERGView and Excel. Both a-wave and b-wave amplitude and implicit time were averaged for the three treatment groups. Data represent the average ± SEM from four observations.

The toxicity of PEDF peptides were also evaluated in our retinal astrocytes (RAC), retinal endothelial cells (REC), retinal pericytes (RPC), ChEC, and choroidal pericytes (ChPC). The isolation and culture of these cells have been described by us (Gurel et al., 2014; Farnoodian et al., 2018). Various cell types were incubated with indicated concentration of peptides and cell viability was assessed after 48 h using the CellTiter 96® Non-Radioactive Cell Proliferation Assay (MTT) as recommended by the supplier (G5421,Promega, Madison, WI). The data is normalized to control treated cells and shows mean ± SEM from three independent observations.

2.11. Rabbit Eye Safety

The following experiments were approved by Northwestern IACUC (Protocol IS00000364). IVT injections (30 μL) of 18 mM PEDF 336 dissolved in 1:1, v:v isotonic saline to Avastin vehicle (10 kDa MWCO ultrafiltrate of 25 mg/mL Avastin) to give 9 mM final peptide concentration, were carried out under anesthesia in 3–4 kg New Zealand white rabbits. Dose was selected as highest attainable stable concentrations, freshly delivered in 30 μL, to approximate Avastin volumes currently injected in patient eyes, rather than to simulate indeterminate mouse IVT exposure from 2 μL injections. Controls included corresponding 12.5 mg/mL Avastin and vehicle-only (n=4). Needle tip (27 Ga 6.0 mm) was positioned 4 to 5 mm posterior to the limbus, directed backward at approximately 45° and pushed through the sclera towards the center of vitreous, with injection posterior to the lens. Eyes were enucleated on day 14 after euthanasia. They were fixed and slides prepared for light microscopic examination following standard techniques. Examination included the cornea, limbus, sclera ciliary body, lens choroid, retina and optic nerve.

3. Results

3.1. Peptide Truncation and Modification

PEDF exerts its anti-angiogenic activity by killing growth factor-activated EC (Zhang et al., 2016). Three active peptide analogs and an inactive 14-mer comprising segments of the PEDF 34-mer sequence, are shown in Figure 1A as reported (Bernard et al., 2009; Mirochnik et al., 2009). Figure 1B shows a portion of the x-ray crystallographic backbone ribbon structure of PEDF (Simonovic et al., 2001) in which the helical 34-mer is seen at the surface, also with a smaller portion in this region expanded. This shortened essential sequence was deduced from results of our testing of synthetic peptides described in Table 1, anti-angiogenic potency measured as EC_{50} for maximal apoptosis of VEGF-stimulated EC. An active 9-mer (PEDF 860) from within PEDF P18, overlapping the more N-terminal 25-mer (Figure 1A) was identified where 2 proximal and 7 distal residues of P18 are removed, displaying 60 nM EC_{50}. Further distal shortening or N-terminal glutarate appendage had only modest effect upon this activity as seen in PEDF 862 and PEDF 406. However compensating the extra anionic charge in PEDF 406 by replacement of internal Asp by Asn in PEDF 427 improved potency to 15 nM. Figure 1C shows VEGF and dose-dependence, also that adipic replacement and shortening of Sar-Gly to Sar in PEDF 336 yields a more potent nonapeptide. C-terminal truncated and Pro-ethylamide capped PEDF 276 and PEDF 335 both improve on the potency of their larger parent peptides. The apoptotic and dose responses of these last 5 peptides are shown and compared in Figure 1C, D, E. improvements by amino acid substitutions, deletions and N-terminal modifications are summarized in Table 1.

3.2. Capillary Sprouting in Explants

When early leads PEDF 406 and PEDF 427 were tested in a model of CNV they showed trends toward inhibition, results were not statistically significant. As a secondary screen for choroidal angiogenic inhibition these short PEDF peptides were tested and compared for their *ex-vivo* effect on vascular morphogenesis and sprouting in an ocular vascular bed, using mouse choroidal explants, which retain characteristic cellular milieu and matrix composition. Our results showed that glutaryl-capped decapeptide, PEDF 406 (sarcosine added at position 1), inhibited capillary sprouting from VEGF-stimulated mouse choroidal explants (Figure 2A,B). Efficacy of PEDF 427, varying from PEDF 406 by a single amino acid replacement, Asp to Asn in position 4, illustrates the acceptability of neutral substitution. Indeed the quantitative image analysis (Figure 2B) suggests more potent sprouting inhibition with the Asn replacement, consistent with the improved EC apoptotic ranking of PEDF 427 (Table 1).

3.3. CNV amelioration by PEDF Peptides

Thrombospondin-1 (TSP1) derived octapeptide (ABT-898), delivered by IVT injection, has been shown to mitigate laser-induced CNV (Wang et al., 2012). We additionally evaluated Its N-terminal adipic half-amide derivative, TSP-868, synthesized as a potential prodrug ester precursor (Figure 3A). The above un-commercialized sequences are covered by patent (US 7,067,490 B2), assigned to Abbott Laboratories. Importantly, we found that TSP-868 efficacy in CNV was increased by early delivery, when IVT injection preceded laser

induction by 2–5 days, compared with day 0 (day of laser treatment) (Figure 3B). Improved p value with pre-dosed benchmark peptide TSP-868, justified such dosing to enhance statistical significance for subsequent CNV testing of PEDF peptides. More optimized peptides, PEDF 336 and PEDF 335, 2 to3 fold more potent than P18, were sufficiently active to bypass the sprouting screen, moving directly to CNV testing. These were thus injected at day −2, whereby both optimized PEDF peptides (PEDF 336 and PEDF 335) reduced neovascular area by approximately 40% (Figure 3C). Much earlier dosing (day −10 to −14) was not effective (Figure 3B; 6B), presumably owing to total clearance of the small peptides.

3.4. Effect of Peptide combination with anti-VEGF antibody on CNV

Octa and nona-peptides, PEDF 335 and PEDF 336, showed significant efficacy, inhibiting mouse CNV (Figure 3C). IVT administration of polyclonal antibody against mouse VEGF (R&D Systems, AF-493-NA), alone and in combination with PEDF 335 or PEDF 336, provided a similar reduction in CNV area. Although there was no increased effect upon addition of peptides to VEGF antibody, the statistical significance was improved by combination treatment with PEDF 336, compared to antibody alone (Figure 4). This very modest effect of combination with anti-VEGF antibody suggests that the PEDF peptides are not synergistic or even additive in benefit when VEGF is simultaneously neutralized. This is consistent with the need for VEGF to observe EC apoptosis by small PEDF peptides (Figure 1C), ie; VEGF primes the EC apoptotic response to PEDF peptides.

3.5. Eye Drop Treatment of CNV Starting Day −7

PEDF 335 is the smaller of the two peptides found active against CNV by a single IVT injection (day −2). Its minimal size and neutral net charge favor its consideration as being capable of trans-corneal penetration, therefore amenable to inhibit CNV via eye drop delivery. While 5 mM saline formulations of PEDF 336 (net charge +1) are stable we observed gelling of 10 mM PEDF 336 on standing after 1–2 weeks. No such instability was seen with PEDF 335 even when > 30 mM. Thus we examined a twice daily (bid) regimen of 5 μL eye drops of 10 mM PEDF 335 for establishing a CNV-inhibiting intraocular environment. Dosing started 7 days before before laser ablation (day −7) to establish an intraocular peptide concentration, eye drops continuing (weekdays only) through day +12, with eye harvest at day +14 (Figure 5A). As shown, while less efficacious than a single IVT injection of 3 mM 335 (1 μL; day −3), weekday eye drop application in mice (10 mM, 5 μL bid) did significantly inhibit CNV, compared with saline vehicle over a 14-day post-laser period, with 33 total eye drops delivered from day −7 through day +12 (Figure 5B,C).

3.6. Prolonged CNV Protection by PEDF 336 Ester NPC-Prodrug

Small modified peptides are expected to have <24 hour IVT half-lives (del Amo et al., 2015), potentially limiting their clinical usefulness. While encouraged by their anti-CNV effect over a 1–2 week range in mice, as monotherapy, their practical clinical use may be of limited value unless slow-release IVT peptide can be provided. We recently described a non-toxic slow-diffusing nanoparticle-peptide conjugate (NPC), relying on 2–3 L-Arg residues as a sole source of cationic charge, adhering to hyaluronate (HA). These studies suggested that NPC of 2-Arg peptides having ζ from +2.0 to +3.5 mV would be expected to have IVT residence $t_{1/2}$ on the order of 3–5 days in rabbit eyes (Melgar-Asensio, 2018), similar to that

of anti-VEGF proteins (bevacizumab, ranibizumab, aflibercept). Free PEDF 336 has +1 net charge but this becomes a +2 charge / peptide when esterified, thus we formed stable carbamate-linked pyrrolidinol conjugates bridged as metastable PE-336 ester prodrugs to CDEX (Figure 6A), for sustained PEDF 336 release, having an average of 40 PEDF 336 esterified per NPC, their properties are shown in Table 2; ζ= +2.3 mV.

The pyrrolidinol bridge was chosen after measuring spontaneous hydrolysis rates of various amino-alkoxy esters in carbamate linkage. We found that pyrrolidine reacted efficiently with activated CDEX, compared with other amines, and that carboxylic esters of 3-hydroxypyrrolidine carbamates hydrolyzed slowly, $t_{1/2}$ >30 days under physiologic conditions. We demonstrated that CDEX prodrug NPC releases free PEDF 336 with $t_{1/2}$ = 35 days at pH 7.4, 37°C (Figure 6A). A long duration study in CNV was then carried out, with IVT injection of sterile-filtered NPC, pre-laser treatment, at day −14. A free PEDF 336 dose of 4 nmoles in 2 μL was compared to 2 μL of a mixture delivering 2 nmol PEDF 336 and 1.3 nmol NPC prodrug peptide. While a trend of CNV inhibition was seen with free peptide alone, this was not statistically significant. By contrast, the mixture containing NPC (Figure 6B) caused significant CNV decrease, based on improved p value. These data indicate that the peptide ester prodrug conjugation to NP, our original rationale for dicarboxylate modification, enables sustained delivery in the vitreous via extended residence of NPC.

3.7. Mouse Eye Safety of PEDF 335 and 336 Peptides

The impact of peptides on retinal function was assessed by ERG analysis as detailed in Methods. Figure 7A shows the ERG analysis of mice two-weeks after receiving a single injection (2 μL of 2 mM) PEDF 335 and 336 peptides or BSS (control). Amplitude of a-wave and b-wave for 10 cd.s/m^2 flash intensity showed the increased response for PEDF 335 compared to control (P=0.01432 and 0.03509, respectively). We did not observe significant difference between control and PEDF 336 for 10 cd.s/m^2 (P=0.6055 a-wave and 0. 2761 b-wave). Both PEDF 335 and 336 appeared to preserve or slightly enhance retina function. We next examined the impact of peptide treatment on histological integrity of eyes from mice treated with different peptides. Following ERG analysis the eyes were harvested and histological preparation were examined in a masked fashion (Figure 7A). No abnormality in the organization and histological pattern of retinas prepared from different groups was seen at up to 8 μg peptide alone (PEDF 335 or PEDF 336) injected.

3.8. Cytotoxicity of PEDF Peptides

To further assess the impact of PEDF peptides on ocular cells integrity, we exmined the effects of PEDF 335 and PEDF 336 peptides on the viability of three retinal and two choroidal cell lines. Figure 7B shows the effect of PEDF peptides on viability of these cells. No cytotoxicity was detected below 50 μM with any peptide over 48 h. PEDF 335 treatment up to 100 μM showed no significant inhibition of growth for any of these cell types although a trend to growth inhibition in ChEC was seen at 100 μM. PEDF 336 treatment at 100 μM gave approximately 40% reduction in growth, only of ChEC, with modest (<20%) inhibition of RPC at 50 and 100 μM.

3.9. Rabbit eye safety of PEDF Peptides

Before eye drop delivery of peptide 335 to mice, we carried out a safety study in 6 rabbits, where each eye was dosed bid with 50 μL eye drops (10 mM PEDF 335, saline, pH 7) over 12 consecutive days. No irritation or discomfort was observed. Neither inflammatory cells nor other abnormalities were seen on histopathologic examination of 4 eyes resected at 2 weeks after IVT injection of 270 μg PEDF 336, with no difference compared to Avastin or vehicle controls.

4. Discussion

Two important RPE-expressed proteins, that resist neo-angiogenesis in human eyes are PEDF and TSP1. PEDF and its active 18 to 34-mer overlapping surface peptides yielded promising preclinical results, blocking angiogenesis in animal models of neoplastic or ocular disease. However these large peptides remain impractical for clinical use. Peptides of this size remain costly to synthesize and potentially immunogenic, as determined by using open online software (http://imed.med.ucm.es/Tools/antigenic.pl). These larger peptides are not readily amenable to polymeric carrier attachment and release for extended action in the vitreous.

We previously showed potent CNV mitigating activity of an 8-aa TSP1 mimetic peptide, (ABT-898), containing a single D-Ile residue (Wang et al., 2012), by day 0 IVT injection in the same model used here. Seeking an ester prodrug precursor of this peptide for sustained release delivery, we generated the benchmark adipate octapeptide analog (TSP-868) described here (Figure 3A), with more statistically significant anti-CNV activity, when IVT injection preceded laser induction by 2–5 days (Figure 3B). By systematic truncation and similar dicarboxylate modification of the PEDF P18 sequence (Mirochnik et al., 2009), we defined an active 8–10 aa sequence within the PEDF-derived 34-mer. The latter comprises a surface-exposed alpha-helix, as determined by x-ray crystal structure analysis of PEDF protein (Bernard et al., 2009; Simonovic et al., 2001). Improved potency was achieved by compensating the appended negative adipate charge via substitution of an internal Asp residue by Asn. Sequence optimization (Table 1) gave N-terminal adipic 8 and 9-mers (PEDF 335 and 336), with respective net charges of 0 and +1, each with significant CNV-inhibitory activity when IVT-injected 2–5 days pre-laser induction (Figure 3C). No safety issues were discerned by histopathology or ERG upon PEDF 336 injection in mouse eyes, nor was histopathology seen in rabbit eyes with combined PEDF 336 / Avastin injection. No corneal irritation was observed with bid eye drops of PEDF 335 in mice or rabbits.

Several receptors have been suggested as mediating PEDF antiangiogenic activity, including PPAR-γ and adipose triglyceride lipase (Biyashev et al., 2010; Gao et al., 2017), although direct high-affinity binding of the 34-mer parent peptide, from which our much smaller peptides are derived, has only been directly observed for the non-integrin 67kDa laminin receptor, 67LR (Bernard et al., 2009). First discovered through its binding of Ln β1 chain pentapeptide YIGSR, the 67LR-Ln interaction drives angiogenesis and local proteolytic generation of Ln motility fragments, the latter was disrupted by synthetic YIGSR peptide (Grant et al., 1990; Ardini et al., 2002). 67LR was induced in newborn mouse retina during oxygen-induced ischemic retinopathy (OIR) (Stitt et al., 1998), neovascularization was

mitigated by systemic administration of an YIGSR-containing nonapeptide, or of an analogous epidermal growth factor decapeptide (YSGDR), that also binds 67LR (Nelson et al., 1996; Gebarowska et al., 2002). Each of the OIR-inhibiting peptides contains a Tyr residue separated by three amino acids from a distal Arg residue, a motif repeated in the PEDF 34-mer sequence spanning G42 to S50 (G**Y**DLY**R**VRS), where the side chains of **Y**43 and **R**47 are both seen from the x-ray crystal structure to point outward in the same water-exposed quadrant of an α-helix under a flexible flap of unstructured sequence (Glu270-Glu276, Figure 1B). The same motif occurs in all peptides listed in Table 1.

Synthetic YIGSR peptides have been studied in cells presenting 67LR, and typically display activity in the 2–20 μM range (Gopalakrishna et al., 2018; Yu et al., 2009). The 67LR interactions with Ln and with PEDF are of much higher affinity, as are those of our potent small peptides, the simplest of which (PEDF 335) has only a single Arg residue. This leads us to hypothesize that the alignment of the Tyr and distal Arg side-chains in a critical α-helix are essential to optimize 67LR binding, although the secondary structure of YIGSR in Ln β1 remains undefined. PEDF may have evolved as a matrix component to oppose 67LR stimulation of basement membrane invasion through 67LR-dependent proteolytic degradation of Ln β1 chains. PEDF's surface 34-mer would thereby inhibit migration of ChEC through Bruch's membrane, which contains Ln-111 (Alsenbrey et al., 2006). Several studies showed that 67LR contributes to PEDF bio-activity (Matsui et al., 2014; Gong et al., 2014). Binding of 67LR ligands, including YIGSR and green tea catechins, to 67LR on cancer cells is known to impede both matrix invasion and leads to increased apoptosis, the latter induced through 67LR endocytosis (Kumazoe et al., 2013). The percent EC population in G2/M, after activation by VEGF, was decreased 2-fold upon addition of 67LR ligands (Chu et al., 2018), as such catechins also attenuated induced EC inflammatory cytokines and adhesion molecules (Byun E-B et al., 2014) via decreased toll-like receptor-4 (TLR4). Macrophage recruitment and polarization have been shown to play a role in OIR neovascularization, these are dampened by PEDF (Gao et al., 2017). 67LR ligation has been shown to downregulate macrophage activation, as with EC, via reduction in TLR4 (Byun E-H et al., 2010). The CNV-mitigating peptides are expected to have IVT half-lives of <24 h, yet they decreased CNV measured 16 days after their injection. Prolonged action may reflect intraocular reservoirs or a change in the phenotype of intraocular macrophages, microglia or EC. Further studies will be needed to determine both the mechanism and duration of CNV inhibition.

PEDF 335, our smallest peptide (zero net charge), was active in mitigating mouse CNV by eye drop administration (Figure 5). While unlikely to reach the posterior retina of a larger eye this reveals the potential of PEDF 335 for eye drop use in anterior neovascular disease, which might slow corneal clouding during topical management of keratitis (Austin et al., 2017). Rapid IVT clearance of antiangiogenic agents limits durability of clinical response. Prolonged PEDF delivery, inhibiting an extended CNV mouse model 57 days has recently been achieved through subretinal injection of a multigenic vector. This carried both anti-VEGFA miRNA and PEDF, the latter contributing to potency via remarkably decreased VEGFA (Askou et al., 2019). Our CNV model only permits analysis near +14 days and small PEDF peptides have only short IVT residence as seen in lack of statistically significant

effect with injection at day −14. We therefore explored a nanoparticle (NP) system developed for prolonged IVT residence, utilizing condensed dextran (CDEX)-based carriers. Conjugated stably to peptides where cationic Arg residues slow NPC diffusion, +2 charged peptides (60 / NP) yield NPC that display IVT half-lives on the order of 7 days in rabbit eyes (Melgar-Asensio et al., 2018). Since PEDF 336 itself has a net +2 charge when esterified, we applied the same approach to a metastable bridged conjugate (40 peptides per NP). We described an experiment (Figure 6) where its metastable pyrrolidylester NPC, a prodrug reservoir, showed significant CNV mitigation when injected 14 days prior to laser induction, statistically significant CNV protection was observed 28 days later. While dosed well before the laser insult it can be inferred that peptide released from prodrug NPC remains present long enough to protect against CNV induction. This illustrates potential of anchored peptide ester prodrugs for sustained release treatment of neovascular eye disease.

Lack of anti-VEGF enhancement by combination with PEDF peptides (Figure 4) is consistent with activated VEGF-primed choroidal EC as targets of peptide-induced apoptosis (Figure 1C), suggesting peptides be used when anti-VEGF therapy is ineffective or paused, and not concurrently.

Conclusions

We discovered a pharmacophore, derived from the α-helical surface 34-mer peptide of PEDF, with possibly as few as 5 critical amino acids, a motif known to bind Ln β1 receptor, 67LR. Modifications (**adipic-X**-Y-**N**-L-Y-R-V…) yielded practical, potent, CNV-mitigating peptides of 8–9aa, to act alone or complement anti-VEGF-therapy. These are potential ester prodrugs for extended IVT delivery, and eye drop activity suggests topical application in attenuating corneal neovascularization.

Acknowledgements

This work was supported by an unrestricted award from Research to Prevent Blindness to the Department of Ophthalmology and Visual Sciences, Retina Research Foundation, P30 EY016665, P30 CA014520, EPA 83573701, R24 EY022883, and R01 EY026078. CMS is supported by the RRF/Daniel M. Albert Chair. NS is a recipient of RPB Stein Innovation Award. DMA was supported by an Unrestricted Grant from Research to Prevent Blindness, New York, NY and P30 EY010572 NIH NEI. Zeta potential (ζ) was measured by the Analytical BioNanoTechnology Equipment Core (ANTEC) of Simpson Querrey Institute (SQI) at Northwestern University (NU), Chicago, IL. Rabbit eye drop delivery, also rabbit IVT injections and eye resections were performed by the NU Developmental Therapeutics Core (DTC), Evanston, IL.

References

Alsenbrey S, Zhang M, Bacher D, Yee J, Brunken WJ, Hunter DD, 2006 Retinal pigment epithelial cells synthesize laminins, including laminin 5, and adhere to them through alpha3- and alpha6-containing integrins. Invest Ophthalmol Vis Sci. 47 (12),5537–5544. 10.1167/iovs.05-1590 [PubMed: 17122146]

Amaral J, Becerra SP, 2010 Effects of human recombinant PEDF protein and PEDF-derived peptide 34-mer on choroidal neovascularization. Invest Ophthalmol Vis Sci. 51 (3), 1318–1326. 10.1167/iovs.09-4455 [PubMed: 19850839]

Ardini E, Sporchia B, Pollegioni L, Modugno M,Ghirelli C, Castiglioni F,Tagliabue E, Menard S, 2002 Identification of a novel function for 67-kDa laminin receptor: increase in laminin degradation rate and release of motility fragments. Canc Res. 62, 1321–1325. https://www.ncbi.nlm.nih.gov/pubmed/11888899

Askou A,L, Alsing S, Benckendorff JNE, Holmgaard A, Jacob Giehm Mikkelsen JG, Aagaard L, Bek T, Thomas J, Corydon TJ 2019 Suppression of choroidal neovascularization by AAV-based dual-Acting antiangiogenic gene therapy. Mol Ther Nucleic Acids. 16, 38–50. 10.1016/j.omtn.2019.01.012 [PubMed: 30825671]

Austin A, Lietman T, Rose-Nussbaumer J, 2017 Update on the management of infectious keratitis. Ophthalmol.124 (11), 1678–1616. 10.1016/j.ophtha.2017.05.012

Bernard A, Gao-Li J, Franco C-A, Bouceba T, Huet A, Li Z, 2009 Laminin receptor involvement in the anti-angiogenic activity of pigment epithelium-derived factor. J Biol Chem. 284 (16), 10480–10490. 10.1074/jbc.M809259200 [PubMed: 19224861]

Bhutto IA, McCleod DS, Hasegawa T, Kim SY, Merges C, Tong P, Lutty GA, 2006 Pigment epithelium-derived factor (PEDF) and vascular endothelial growth factor (VEGF) in aged human choroid and eyes with age-related macular degeneration. Exp Eye Res 82 (1), 99–110. 10.1016/j.exer.2005.05.007 [PubMed: 16019000]

Biyashev D, Veliceasa D, Kwiatek A, Sutanto. MM, Cohen RN, Volpert OV, 2010 Natural angiogenesis inhibitor signals through Erk5 activation of peroxisome proliferator-activated receptor gamma (PPARgamma). J Biol Chem. 285 (18), 13517–24. 10.1074/jbc.M110.117374 [PubMed: 20185831]

Byun E-B, Yang M-S, Kim J-H, Song D-S, Lee B-S, Park J-N, Park S-H, Park C, Jung P-M, Sung N-Y, Byun E-H, 2014 Epigallocatechin-3-gallate-mediated Tollip induction through the 67-kDa laminin receptor negatively regulating TLR4 signaling in endothelial cells. Immunobiology 219 (11), 866–872. 10.1016/j.imbio.2014.07.010 [PubMed: 25109435]

Byun E-H, Fujimura Y, Yamada K, Tachibana H, 2010 TLR4 signaling inhibitory pathway induced by green tea polyphenol epigallocatechin-3-gallate through 67-kDa laminin receptor. J Immunol. 185 (1), 33–45. 10.4049/jimmunol.0903742 [PubMed: 20511545]

Chu KO, Chan KP, Chan SO, Ng TK, Jhanji V, Wang CC, Pang CP, 2018 Metabolomics of green-tea catechins on vascular-endothelial-growth-factor-stimulated human-endothelial-cell survival. J Agric Food Chem. 2018; 66(48):12866–12875. 10.1021/acs.jafc.8b05998 [PubMed: 30406651]

del Amo EM, Vellonen KS, Kidron H, Urtti A, 2015 Intravitreal clearance and volume of distribution of compounds in rabbits: In silico prediction and pharmacokinetic simulations for drug development. Eur J Pharm Biopharm. 95 (Pt B), 215–26. 10.1016/j.ejpb.2015.01.003 [PubMed: 25603198]

Duh EJ, Yang HS, Suzuma I, Miyagi M, Youngman E, Mori K, Katai M, Yan L, Suzuma K, West K, Davarya S, Tong P, Gehlbach P, Pearlman J, Crabb JW, Aiello LP, Campochiaro PA, Zack DJ, 2002 Pigment epithelium-derived factor suppresses ischemia-induced retinal neovascularization and VEGF-induced migration and growth. Invest Ophthalmol Vis Sci. 43 (3), 821–829. https://www.ncbi.nlm.nih.gov/pubmed/11867604 [PubMed: 11867604]

Farnoodian M, Wang S, Dietz J, Nickells RW, Sorenson CM, Sheibani N, 2017 Negative regulators of angiogenesis: Important targets for treatment of exudative AMD. Clin Sci (Lond). 131 (15), 1763–1780. 10.1042/CS20170066 [PubMed: 28679845]

Farnoodian M, Sorenson CM, Sheibani N, 2018 PEDF expression affects the oxidative and inflammatory state of choroidal endothelial cells. Am J Physiol Cell Physiol. 314 (4), C456–C472. 10.1152/ajpcell.00259 [PubMed: 29351407]

Filleur S, Volz K, Nelius T, Mirochnik Y, Huang H, Zaichuk TA, Aymerich MS, Becerra SP, Yap R, Veliceasa D, Shroff EH, Volpert OV, 2005 Two functional epitopes of pigment epithelial-derived factor block angiogenesis and induce differentiation in prostate cancer. Cancer Res. 65 (12), 5144–5152. 10.1158/0008-5472.CAN-04-3744 [PubMed: 15958558]

Gao S, Li C, Zhu Y, Wang Y, Sui A, Zhong Y, Xie B, Shen X, 2017 PEDF mediates pathological neovascularization by regulating macrophage recruitment and polarization in the mouse model of oxygen-induced retinopathy. Sci Rep. 7, 42846 10.1038/srep42846 [PubMed: 28211523]

Gebarowska D, Stitt AW, Gardiner TA, Harriott P, Greer B, Nelson J, 2002 Synthetic peptides interacting with the 67-kd laminin receptor can reduce retinal ischemia and inhibit hypoxia-induced retinal neovascularization. Am J Pathol. 160 (1), 307–313. 10.1016/S0002-9440(10)64374-X [PubMed: 11786424]

Gemenetzi M, Lotery AJ, Patel PJ, 2017 Risk of geographic atrophy in age-related macular degeneration patients treated with intravitreal anti-VEGF agents. Eye (Lond). 31,1–9. 10.1038/eye.2016.208 [PubMed: 27716750]

Gong Y, Li J, Sun Y, Fu Z, Liu C-H, Evans L,Tian K, Saba N, Fredrick T, Morss P, Chen J, Smith LEH, 2015 Optimization of an Image-Guided Laser-Induced Choroidal Neovascularization Model in Mice. PLoS ONE 10(7), e0132643 10.1371/journal.pone.0132643 [PubMed: 26161975]

Gong Q, Qiu S, Li S, Ma Y, Chen M, Yao Y, Che D, Feng J, Cai W, Ma J, Yang X, Gao G, Yang Z, 2014 Proapoptotic PEDF functional peptides inhibit prostate tumor growth–a mechanistic study. Biochem Pharmacol. 92, 425–437. 10.1016/j.bcp.2014.09.012 [PubMed: 25261795]

Gopalakrishna R, Gundimeda U, Zhou S, Bui H, Davis A, McNeill T, Mack W, 2018 Laminin-1 induces endocytosis of 67KDa laminin receptor and protects Neuroscreen-1 cells against death induced by serum withdrawal. Bioch Biophys Res Commun. 495, 230–237. 10.1016/j.bbrc.2017.11.015

Grant DS, Kleinman HK, Martin GR, 1990 The role of basement membranes in vascular development. Ann NY Acad Sci. 588, 61–72. 10.1111/j.1749-6632.1990.tb13197.x [PubMed: 2192650]

Gurel Z, Zaro BW, Pratt MR, Sheibani N, 2014 Identification of O-GlcNAc modification targets in mouse retinal pericytes: Implication of p53 in pathogenesis of diabetic retinopathy. PLoS One 9 (5): e95561 10.1371/journal.pone.0095561 [PubMed: 24788674]

Jimenez B, Volpert OV, Crawford SE, Febbraio M, Silverstein RL, Bouck N, 2000 Signals leading to apoptosis-dependent inhibition of neovascularization by thrombospondin-1. Nat Med. 6 (1), 41–48. 10.1038/71517 [PubMed: 10613822]

Jonasson F, Fisher DE, Eiriksdottir G, Sigurdsson S, Klein R, Launer LJ, Harris T, Gudnason V, Cotch MF, 2014 Five-year incidence, progression, and risk factors for age-related macular degeneration: the age, gene/environment susceptibility study. 121 (9),1766–1772. 10.1016/j.ophtha.2014.03.013

Kumazoe M, Sugihara K, Tsukamoto S, Huang Y, Tsurudome Y, Suzuki T, Suemasu Y, Ueda N,Yamashita S, Kim Y, Yamada K, Tachibana H, 2013 67-kDa laminin receptor increases cGMP to induce cancer-selective apoptosis. J. Clin. Invest. 123 (2), 787–799. 10.1172/JCI64768 [PubMed: 23348740]

Li H, Liu W, Sorenson CM, Sheibani N, Albert DM, Senanayake T, Vinogradov S, Henkin J, Zhang HF, 2017 Sustaining intravitreal residence with L-arginine peptide-conjugated nanocarriers. Invest Ophthalmol Vis Sci. 58(12): 5142–5150. 10.1167/iovs.17-22160 [PubMed: 28986592]

Loegl J, Nusshaumer E, Hiden U, Majali-Martinez A, Ghaffari-Tabrizi -Wizy N, Cvitic S, Lang I, Desoye G, Huppertz B, 2016 Pigment epithelium-derived factor (PEDF): a novel trophoblast-derived factor limiting feto-placental angiogenesis in late pregnancy. Angiogenesis 19 (3), 373–388. 10.1007/s10456-016-9513-x [PubMed: 27278471]

Longeras R, Farjo K, Ihnat M, Ma J-X, 2012 A PEDF-derived peptide inhibits retinal neovascularization and blocks mobilization of bone marrow-derived endothelial progenitor cells. Experimental Diabetes Res. 2012, 51846 10.1155/2012/518426

Matsui T, Higashimoto Y, Yamagishi S-i., 2014 Laminin receptor mediates anti-inflammatory and antithrombotic effects of pigment epithelium-derived factor in myeloma cells. Biochem Biophys Res Commun. 443, 847–85. 10.1016/j.bbrc.2013.12.060 [PubMed: 24342618]

Melgar-Asensio I, Kandela I, Aird F, Darjatmoko SR, Cristobal de los Rios C, Sorenson CM, Albert DM, Sheibani N, Henkin J, 2018 Extended intravitreal rabbit eye residence of nanoparticles conjugated with cationic arginine peptides for intraocular drug delivery: in vivo imaging. Invest Ophthalmol Vis Sci. 59(10), 4071–4081. 10.1167/iovs.18-24087 [PubMed: 30098194]

Mirochnik Y, Aurora A, Schulze-Hoepfner FT, Deabes A, Shifrin V, Beckmann R, Polsky C, Volpert OV, 2009 Short PEDF-derived peptide inhibits angiogenesis and tumor growth. Clin Cancer Res.15(5),1655–1663. 10.1158/1078-0432.CCR-08-2113 [PubMed: 19223494]

Nelson J, Scott WN, Allen WE, Wilson DJ, Harriott P, McFerran NV, Walker B, 1996 Murine epidermal growth factor peptide (33–42) binds to a YIGSR-specific laminin receptor on both tumor and endothelial cells. J Biol Chem. 271(42), 26179–26186. 10.1074/jbc.271.42.26179 [PubMed: 8824265]

Ogata N, Nishikawa M, Nishimura T, Mitsuma Y, Matsumura M, 2002 Unbalanced vitreous levels of pigment epithelium-derived factor and vascular endothelial growth factor in diabetic retinopathy.

Am J Ophthalmol. 134(3), 348–353. https://www.ncbi.nlm.nih.gov/pubmed/12208245 [PubMed: 12208245]

Saishin Y, Silva RL, Saishin Y, Kachi S, Aslam S, Gong YY, Lai H, Carrion M, Harris B, Hamilton M, Wei L, Campochiaro PA, 2005 Periocular gene transfer of pigment epithelium-derived factor inhibits choroidal neovascularization in human-sized eye. Human Gene Therapy 16(4), 473–478. 10.1089/hum.2005.16.473 [PubMed: 15871678]

Shahi PK, Liu X, Aul B, Moyer A, Pattnaik A, Denton J, Pillers D-AM, Pattnaik BR, 2017 Abnormal Electroretinogram after Kir7.1 Channel Suppression Suggests Role in Retinal Electrophysiology. Sci Rep. 7: 10651 10.1038/s41598-017-11034-1 [PubMed: 28878288]

Shao Z, Friedlander M, Hurst CG, Cui Z, Pei DT, Evans LP, Juan AM, Tahiri H,Duhame l.F., Chen J, Sapieha P, Chemtob S, Joyal JS, Smith. 2013 Chroroid sprouting assay: an *ex-vivo* model of microvascular angiogenesis. PLOS One 8(7), e69552 10.1371/annotation/c6b85ec4-996d-4daf-863a-44260a888470 [PubMed: 23922736]

Simonovic M, Gettins PGW, Volz K, 2001 Crystal structure of human PEDF, a potent anti angiogenic and neurite growth-promoting factor. Proc Natl Acad Sci USA. 98(20),11131–11135. 10.1073/pnas.211268598 [PubMed: 11562499]

Stitt AW, McKenna D, Simpson DA, Gardiner TA, Harriott P, Archer DB, Nelson J, J.,1998 The 67-kd laminin receptor Is preferentially expressed by proliferating retinal vessels in a murine model of ischemic retinopathy. Am J Pathol. 152(5),1359–1365. https://www.ncbi.nlm.nih.gov/pubmed/9588904 [PubMed: 9588904]

Sugioka K, Saito A, Kusaka S, Kuniyoshi K, Shimomura Y, 2017. Identification of vitreous proteins in retinopathy of prematurity. Biochem Biophys Res Commun. 488, 483–488. 10.1016/j.bbrc.2017.05.067 [PubMed: 28502635]

Sulaiman RS, Merrigan S, Quigley J, Qi X, Lee B, Boulton ME, Kennedy B, Seo S-Y, Corson TW, 2016 A novel small molecule ameliorates ocular neovascularisation and synergises with anti-VEGF therapy. Sci Rep. 6, 25509 10.1038/srep25509 [PubMed: 27148944]

Uno K, Bhutto IA, McCleod DS, Merges C, Lutty GA, 2006 Impaired expression of thrombospon din-1 in eyes with age related macular degeneration. Br J Ophthalmol. 90, 48–54. 10.1136/bjo.2005.074005 [PubMed: 16361667]

Wang S, Sorenson CM, Sheibani N, 2012 Lack of thrombospondin-1 and exacerbation of choroidal neovascularization. Arch Ophthalmol. 130(5), 615–620. 10.1001/archopthalmol.2011.1892 [PubMed: 22232368]

Wen JC, Reina-Torres E, Sherwood JM, Challa P, Liu KC, Li G, Chang JYH, Cousins SW, Schuman SG, Mettu PS, Stamer WD, Overby DR, Allingham RR, 2017 Intravitreal anti-VEGF injections reduce aqueous outflow facility in patients with neovascular age-related macular degeneration. Invest Ophthalmol Vis Sci. 58, 1893–1898. 10.1167/iovs.16-20786 [PubMed: 28358961]

Willis JR, Doan QV, Gleeson M, Haskova Z, Ramulu P, Morse L, Cantrell RA, 2017 Vision-Related Functional Burden of Diabetic Retinopathy Across Severity Levels in the United States. JAMA Ophthalmol. 135(9), 926–932. 10.1001/jamaophthalmol.2017.2553 [PubMed: 28750122]

Wolf A, Kampik A, 2014 Efficacy of treatment with ranibizumab in patients with wet age-related macular degeneration in routine clinical care: data from the COMPASS health services research. Graef Arch Clin Exp Ophthalmol. 252(4), 647–655. 10.1007/s00417-013-2562-6

Yassai M, Afsari A, Garlie J, Gorski J, 2002 C-terminal anchoring of a peptide to class II MHC via the P10 residue is compatible with a peptide bulge. J Immunol. 16, 1281–1285. 10.4049/jimmunol.168.3.1281

Yu H-n., Zhang L-c., Yang J-.g, Das UN, Shen S-r., 2009 Effect of tyrosine-isoleucine-glycine-serine-arginine peptide on the growth of human prostate cancer (PC-3) cells in vitro. Eur J. Pharmacol. 616, 251–255. 10.1016/j.ejphar.2009.06.050 [PubMed: 19577562]

Zarubina AV, Gal-Or O, Huisingh CE, Owsley C, Freund KB, 2017 Macular atrophy development and subretinal drusenoid deposits in antivascular endothelial growth factor treated age-related macular degeneration. Invest Ophthalmol Vis Sci. 58, 6038–6045. 10.1167/iovs.17-22378 [PubMed: 29196768]

Zhang H, Wei T, Jiang X, Li Z, Cui H, Pan J, Zhuang W, Sun T, Liu Z, Zhang Z,Dong H, 2016 PEDF and 34-mer inhibit angiogenesis in the heart by inducing tip cells apoptosis via upregulating

PPAR-γ to increase surface FasL. Apoptosis 21, 60–68. 10.1007/s10495-015-1186-1 [PubMed: 26519036]

Highlights

- 18 to 34-mer peptides from Pigment Epithelium-derived Factor (PEDF) are potently anti-angiogenic but impractically large for therapeutic use
- Modified 8 to 9-mer subfragments were discovered here to induce EC apoptosis and inhibit choroidal neovascularization (CNV) via intravitreal (IVT) injection
- IVT peptide combination with anti-VEGF does not enhance efficacy, PEDF 8-mer inhibited CNV as eye drops, may thus have use in corneal neovascularization
- Poly-cationic nanoparticle conjugate of 9-mer shows extended CNV protection

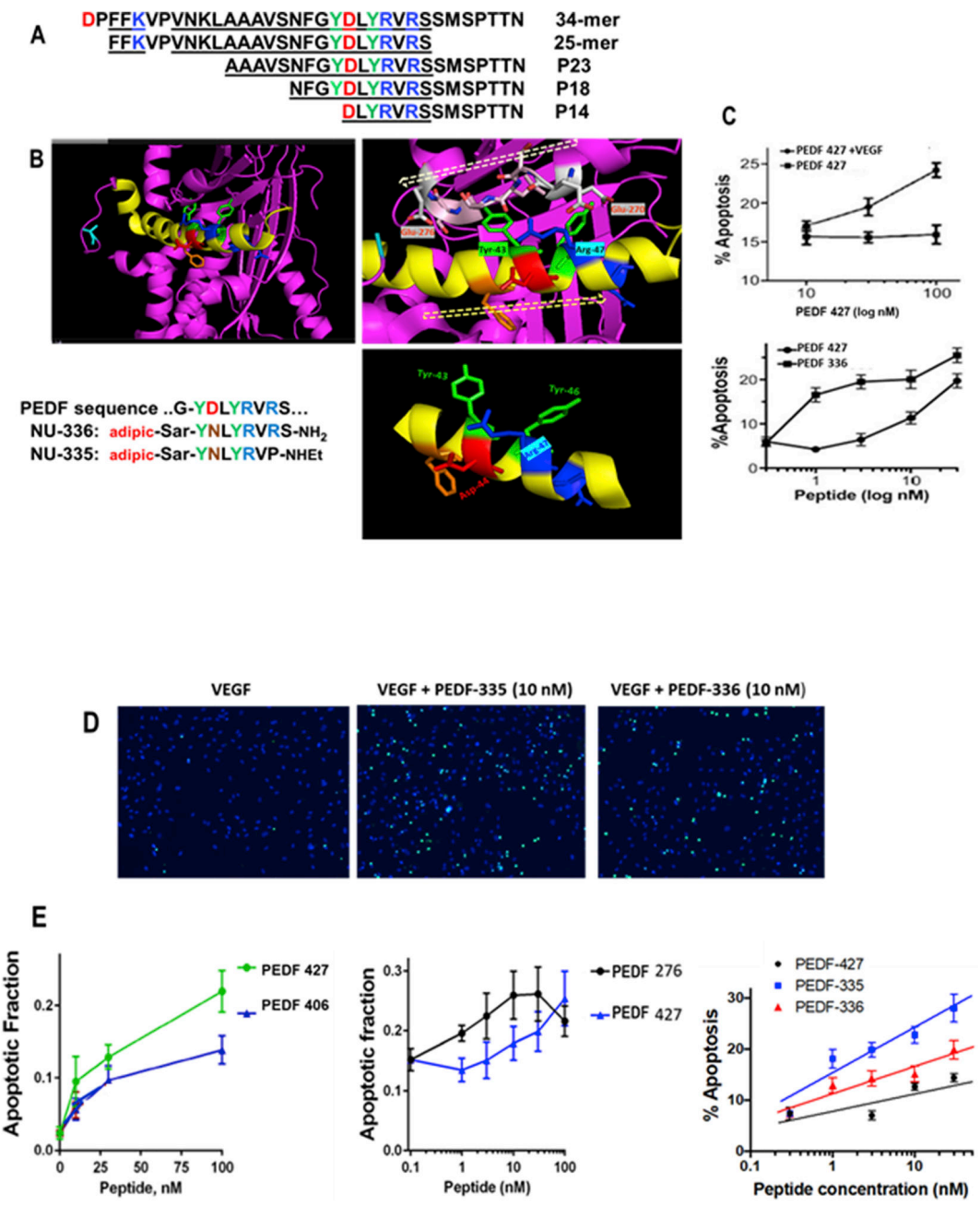

Figure 1. Secondary structure and mimicry of PEDF N-terminal 34-mer peptide.

(A) The active anti-angiogenic, largely α-helical 34-mer extends from Asp-24 to Asn-56 of PEDF (Filleur et al., 2005). An active N-terminal 25-mer therein bound tightly to 67LR (Bernard et al., 2009), and more distal 23-mer and 18-mer (P18) fragments have also been shown active, although a 14-mer starting at Asp44 was inactive (Mirochnik et al., 2009). Amino acid sequences are shown with positively charged residues in blue, negative residues red and Tyr in green, with shaded alpha-helical span from Asn32 through Ser52. (B) The PEDF x-ray crystal structure Protein Data Base PDB ID 1IMV, (Simonovic et al., 2001) is shown as ribbon backbone, the above region highlighted yellow. It is then enlarged from N32-S52, hashed arrow left-to-right tracing N-to-C direction. This reveals Arg47 accessible

to solvent, with Tyr43 partially overlaid by residues 270–276 (EESKLTSE, hashed arrow right-to-left N-to-C direction) in a disordered segment, likely able to move, allowing Tyr43 solvent access. Bottom right panel is the Asn39 to Met51 portion where side chains of Tyr43 and Arg47 are seen on the same helical face, replicated in synthetic peptides shown. (C) Apoptosis assay, as described in section 2.7, shows VEGF requirement, also peptide concentration dependence indicates PEDF 336 improvement over PEDF 427. D) EC apoptosis was detected by in situ TUNEL (green), cell nuclei highligfhted by DAPI (blue) with representative images of EC apoptosis shown. Quantitative analysis performed using Nikon Elements software and percent apoptotic cells calculated for each treatment. A minimum of 8 field per condition (100–300 cells per field) were analyzed. (E) Linear regression plots were generated using Prizm 6 software package. Pairwise and 3-peptide simultaneous comparisons are shown as concentration dependence, leading to the potency ranking in Table 1. Statistical significance was determined using multiple T test ($P<0.0001$).

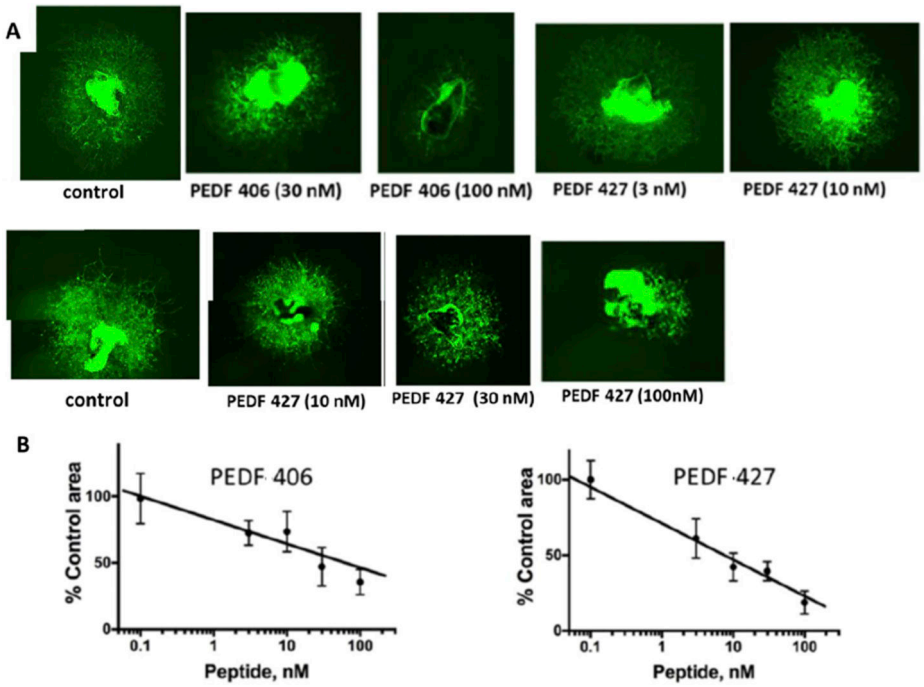

Figure 2. PEDF peptides inhibit choroidal neovascularization *ex vivo*.

Choroidal explants were generated from eyes harvested from C57Bl6 mice that carry eGFP transgene under beta-actin promoter. The explants were embedded in Matrigel drops and cultured in media containing VEGF alone or with increasing concentrations of selected PEDF peptides from Table 1. The explants were observed daily and images were acquired at 6 days endpoint. Composite images were generated for larger vascular areas to evaluate the full vascular area. (A) Representative images of VEGF-stimulated choroidal explants treated with PEDF 406 at increasing concentrations. Similar images were obtained for PEDF 427. (B) Quantitative analysis of the images as shown in A. Sprouting area was measured using ImageJ software and the area of explant subtracted for each image. A minimum of 3 explants were analyzed per data point. Statistical significance was determined using multiple T-test and P value is below 0.0001 for both C and D.

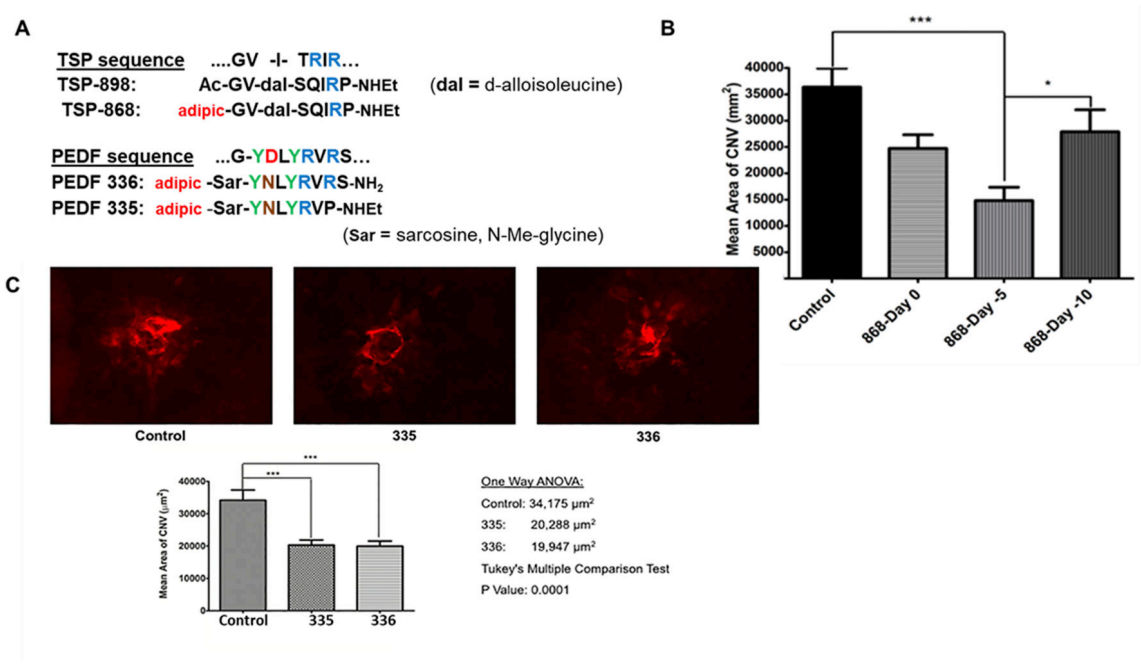

Figure 3. Peptide inhibition of CNV.

(A) TSP1-derived and PEDF-derived test peptide sequences are shown in relation to original protein sequence. Benchmark anti-angiogenic TSP-1 mimetic peptide (ABT-898): Ac-GV-d-alloIle-Ser-Q-I-R-Pro-ethylamide has been shown to inhibit laser-induced mouse CNV (Wang et al., 2012). Substituting N-terminal adipic acid as a half-amide in place of the N-acetyl group gave TSP-868, also displaying anti-CNV activity, with potential capacity to form an adipic half-ester prodrug. (B) TSP-868 (2μL, 2 mM) was compared against balanced salts vehicle at different times of IVT injection where day 0 is the day of laser treatment. CNV mitigation by peptide TSP-868 was significant when 4 ng in 2 μL PBS was IVT-injected on the day of laser, with effect enhanced by injecting at day −2 (not shown) or day −5 before laser treatment. No isignificant inhibition of CNV was evident with injection at day −10. (C) Peptides PEDF 335 and PEDF 336 were IVT injected (2μL, 2 mM) 2 days prior to laser treatment. PEDF-335 and PEDF-336 IVT injection at day −2 significantly decreased CNV by 40–50%, similar inhibition was obtained with injection on day −5 (not shown). In all cases eyes were harvested for CNV analysis at day +14.

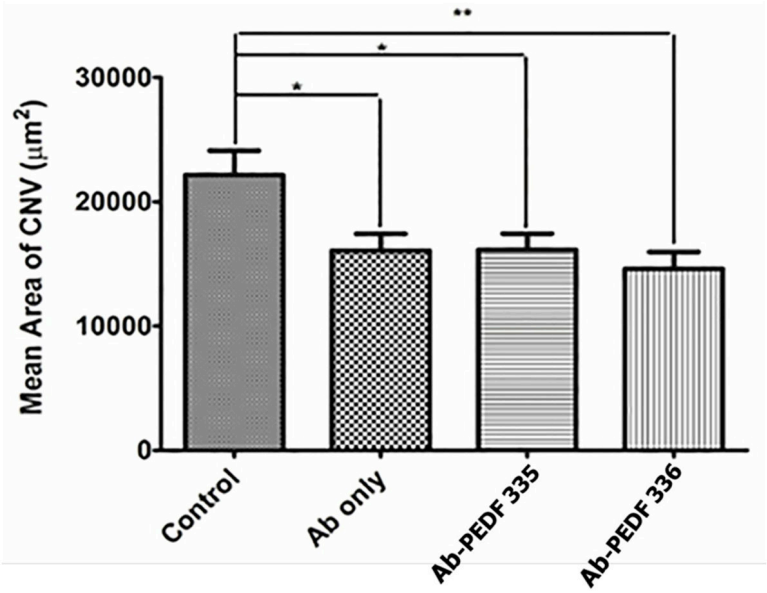

Figure 4. Evaluation of anti-VEGF alone or in combination with PEDF peptides.

Mice were IVT- injected with anti-mouse $VEGF_{164}$ (1 μL of 25 μg/mL alone or in combination with PEDF peptides (1 μL 4 mM peptide in the antibody solution) on day −2. The vehicle was Avastin-vehicle per package insert (trehalose, phosphate, NaCl), and was used for preparing all solutions. Animals were sacrificed on day 14 and RPE/choroidal flatmounts were prepared and stained with anti-ICAM-2 as described under “Methods”.The lesion areas were determined using imageJ. Please note a significant inhibition of neovascularization with antibody alone (*P< 0.05) and similar response with antibody and PEDF-335 (*P< 0.05). Statistical significance was enhanced by PEDF-336 (**P< 0.01).

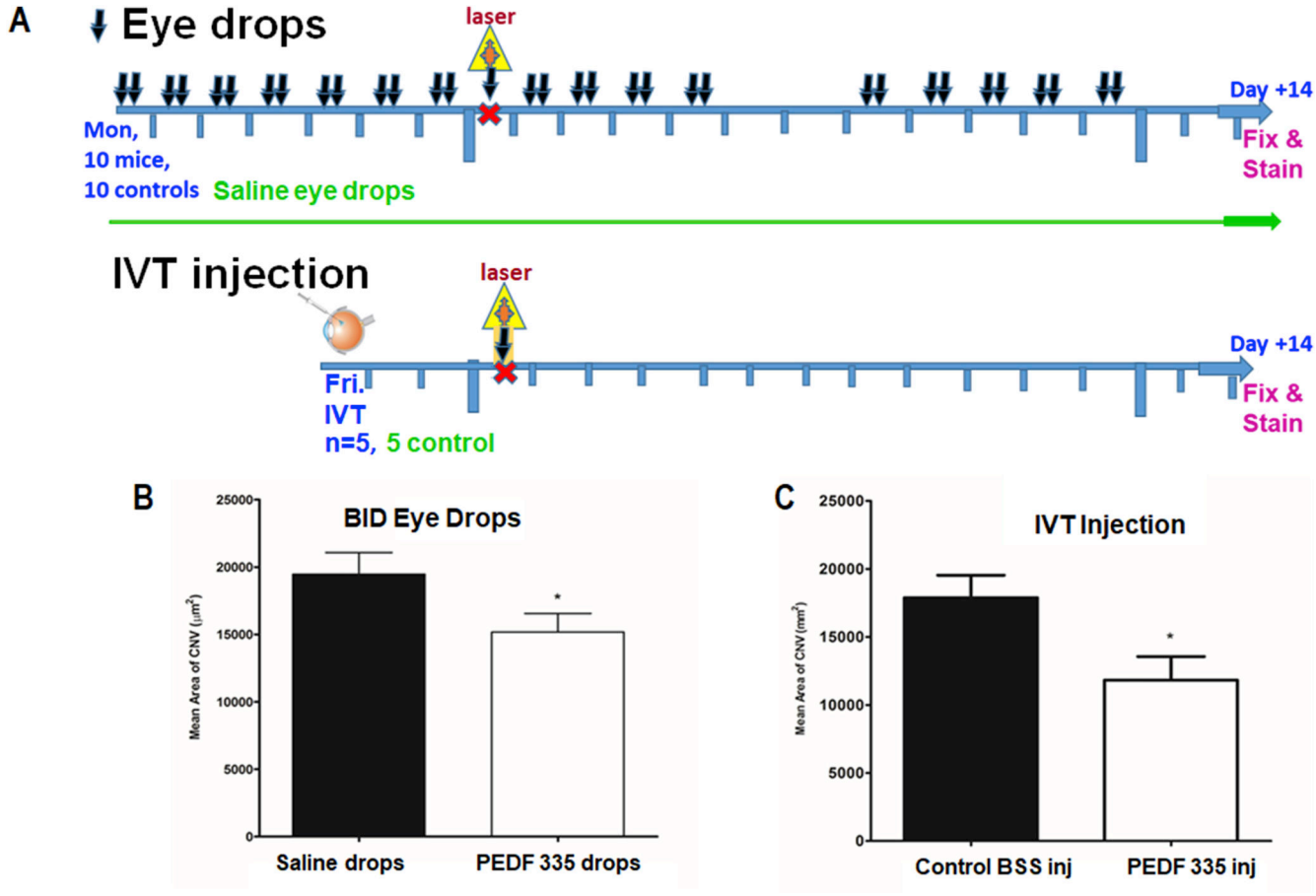

Figure 5. PEDF 335 delivery via eye drops was effective in attenuation of CNV.

Animals (5 per group) received vehical alone or PEDF 335 peptide by one-time IVT injection (1 μL of 4 mM peptide). The topical treatment groups (10 mice / group received 10 mM peptide or saline (5 μL drop, bid, Mon-Fri) starting at day −7. (A) shows the schedule of eye drop or IVT dosing and eye harvest and fixation. Animals were then treated with laser on day 0 and topical delivery of the peptide or saline control drops continued Mon-Fri during the ensuing 14 day period. Animals were then sacrificed and RPE/Choroid flatmounts were stained with ICAM-2 antibody and was determined as described in Methods. (B) Area of vascularization for IVT injection at day −3. (C) Area of vascularization for topical treatment. Inhibition was similarly significant for both treatments, (*P< 0.05).

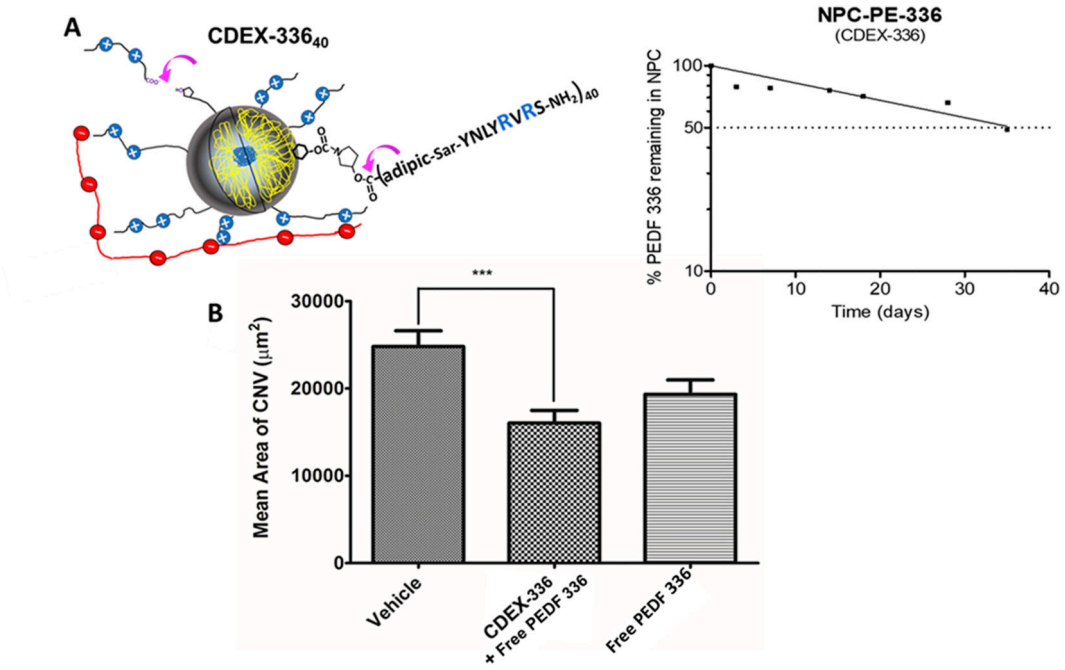

Figure 6. CDEX NPC peptide ester prodrug extends anti-CNV effect.

(A) Pyrrolydyl-3OH ester of PEDF 336 (PE-336), was carbamate-conjugated to glucose OH groups in CDEX, giving prodrug NPC-PE-$(336)_{40}$, with ζ = +2.3 mV (Table 2). (A) Representation at left shows NPC prodrug adherence to IVT HA by multivalent ionic interaction (Melgar-Asensio et al., 2018), purple arrows point to sites of spontaneous ester hydrolysis. Released peptide at 154 days (taken as 95% completion of hydrolysis) and at earlier incubation times was measured via UV spectra of ultrafiltrates. Un-hydrolyzed prodrug ester covalently attached to NPC at these times was: % remaining = 100–100 × (0.295 - OD_{275nm} ultrafiltrate)/(0.295), with calculated release $t_{1/2}$ of 35 +/− 5 days based on one phase exponential decay analysis by GraphPad Prism version 5, GraphPad Software, La Jolla, CA. Semi-log loss of free PEDF 336 is shown on the right under physiological conditions in buffer. (B) IVT injection was carried out 14 days prior to laser induction. For free peptide this was 2 μL containing 4 nmoles of PEDF 336. CDEX-336 injection was 2 μL containing 2 nmoles of free peptide and 1.3 nmoles (1.5 μg) of peptide as prodrug in (4.3 μg NPC), expected daily peptide release approximately 20–30 ng. CNV was estimated as described at 28 days post-injection, only the NPC prodrug mixture showed statistically significant CNV reduction (**P< 0.01).

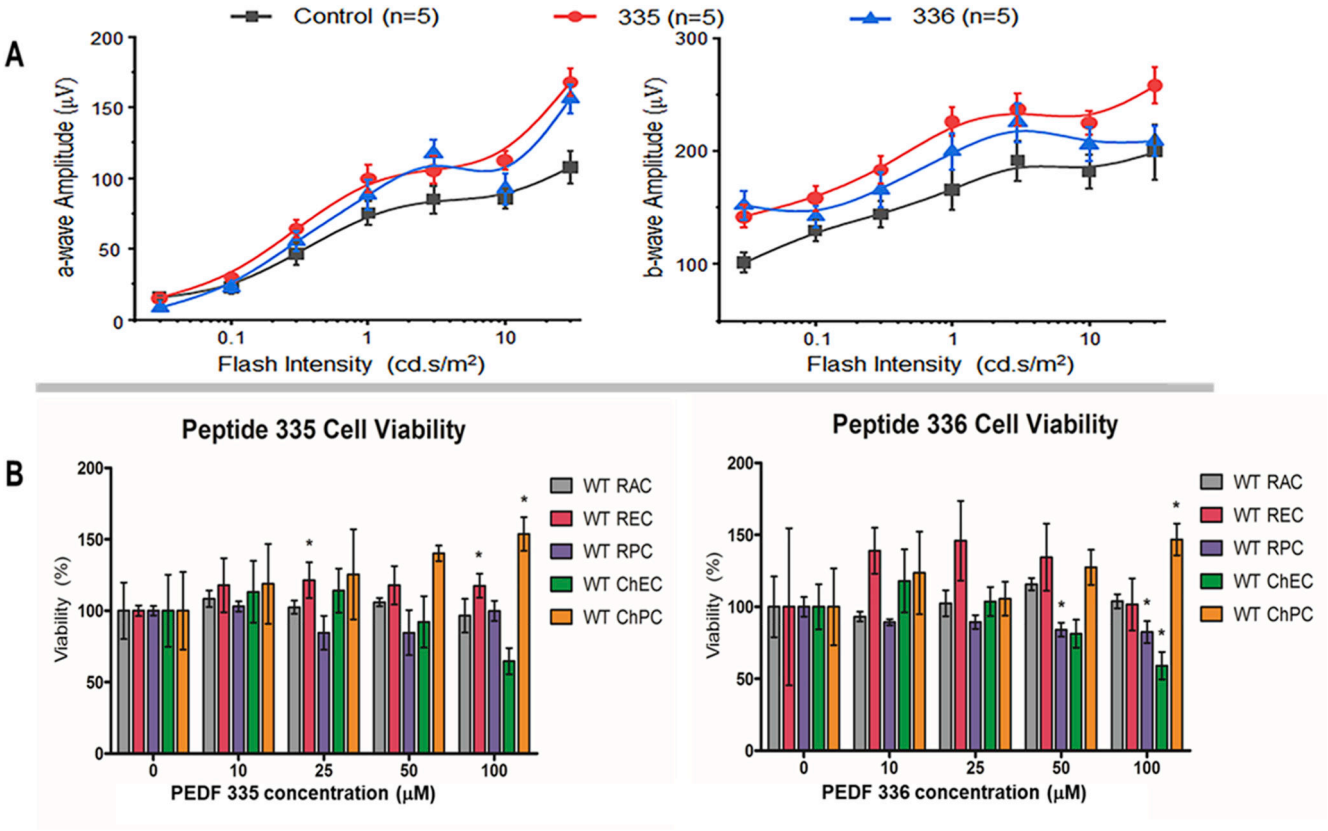

Figure 7. Peptide safety: ERG and cytotoxicity.

(A) Average a- (left panel) and b-wave (right panel) amplitudes are shown in response to increasing flash intensities for mice (5 per group, 10 eyes) after injected with 2 μL of 335 (red circle), 336 (blue triangle) peptide or BSS (black square, balanced salts solution-vehicle control). Data represented as average ± SEM. (B) Cell viability in response to peptide treatments. Various cell types were incubated with indicated concentration of peptides and cell viability was assessed after 48 h using the Cell Titer 96® Non-Radioactive Cell Proliferation Assay (MTT) as recommended by the supplier. The data is normalized to control treated cells and shows mean ± SEM from three independent observations. Abbreviations: RAC, retinal astrocytes; REC, retinal endothelial cells; RPC, retinal pericytes; ChEC, choroidal endothelial cells; ChPC, choropidal pericytes.

Table 1.

Peptide SAR

Sequence	Peptide number	EC_{50}
NFGYDLYRVRSSMSPTTN	**PEDF P18**	10 nM
Ac-**G**Y**D**L**Y**R**V**R**S**-NH_2	**PEDF 860** aa 42–50	60 nM
Ac-**G**Y**D**L**Y**R**V**-NH_2	**PEDF 862** aa 42–48	30 nM
glutaric-**Sar-G**Y**D**L**Y**R**V**R**S**-NH_2	**PEDF 406** glutaric-Sar-PEDF 860	30 nM
glutaric-**Sar-G**Y**NL**Y**R**V**R**S**-NH_2	**PEDF 427** (D44-to-N)-PEDF 406	15 nM
glutaric-**Sar-G**Y**NL**Y**R**V**P**-NHEt	**PEDF 276** (D44-to-N) glutaric-Sar- aa 42–48P-NHEt	7 nM
adipic-**Sar-**Y**NL**Y**R**V**P**-NHEt	**PEDF 335** (D44-to-N) adipic-Sar- aa 43–48-P-NHEt	3 nM
adipic-**Sar-**Y**NL**Y**R**V**R**S**-NH_2	**PEDF 336** (D44-to-N) adipic-Sar- aa 43–50	5 nM

EC_{50} is for apoptosis of VEGF-activated endothelial cells.

Abbreviations: aa: amino acid, Sar: sarcosine (N-methylglycine)

Positive-charged aa in blue; negative-charged aa in red; tyrosine shown in green.

Table 2.

Properties of PE-336 prodrug-CDEX Nanoparticle Conjugate (NPC)

p-nP/CDEX before conjugation	108
% CDEX mass recovered (%)	78
Particle diameter (nm)	178±9
ζ (mV)	+2.3±0.5
PEDF-336 /CDEX (by ultrafiltrate UV)	40
+ charges per 120 kDa NPC	80

PE-336 is the pyrrolidinol ester of PEDF 336. Peptide / NPC was estimated from UV Tyr spectrum (2 Tyr molar extinction of 2,200 at 275 nm). Peptide load of 40 / NPC was obtained by UV spectrum of > 95% hydrolyzed sample (ultrafiltrate, 10kDa MWCO) after incubation 154 days, at 37°C, pH 7.4. Diameter and ζ (zeta potential) of NPC was analyzed by dynamic light scattering and electrophoretic light scattering, respectively (Zetasizer Nano ZsP). *p*-nP (*p*-nitrophenyl groups).